Homodyne In-Phase and Quadrature Detection of Weak Coherent States With Carrier Phase Tracking

Qing Xu, Arturo Arvizu Mondragón, Philippe Gallion, *Senior Member, IEEE*, and Francisco J. Mendieta, *Member, IEEE*

***Abstract*—We present a homodyne receiver structure for the detection of weak coherent states that uses sequential in-phase and quadrature measurements on the received optical signal. This receiver performs the optical carrier phase tracking requiring only a single balanced homodyne detector, by including a postdetection Costas-loop-type feedback, which additionally allows the use of suppressed carrier modulations in the received field, for efficient transmission. We report an experimental interferometric self-homodyne setup for the sequential detection of low photon number, binary phase-modulated optical signals that consist of strongly attenuated laser pulses by using a reference field as the local oscillator with an alternatively switched phase. A Costas loop postdetection subsystem is implemented in discrete time to perform fast real-time optical phase tracking. We also present the experimental results of the homodyne postdetection statistics for received BPSK signals with very low photon numbers, and compare them with the theoretical uncertainty limit. Finally, we conduct bit error rate measurements over a wide range of signal level, as well as a comparison with the standard quantum limit.**

***Index Terms*—Balanced homodyne detection (BHD), coherent detection, in-phase and quadrature measurements, optical Costas loop, optical phase-shift keying (PSK), optical phase synchronization, quantum communications, weak coherent states (WCSs).**

I. Introduction

HOMODYNE optical communications are currently receiving renewed interest due to their unique characteristics of sensitivity to complex amplitude modulations that require substantially lower optical SNR for a given postdetection bit error rate (BER) [1] than the traditional intensity-modulated (IM) ON–OFF keying (OOK) incoherent systems with direct detection. Coherent technologies offer the advantages of a much better spectral efficiency [2], [3], and, when constant envelope modulations are used, they are much more tolerant to nonlinearities in the fiber optic channel [4], [5]. Additionally, for densely multiplexed systems, their highly selective spectral transposition into baseband constitutes an efficient demultiplexing scheme.

Manuscript received February 5, 2009; revised March 26, 2009. First published August 18, 2009; current version published December 3, 2009. This work was supported by the French Government under Project ANR RNRT HQNET.

Q. Xu and P. Gallion are with the Département Communications et Électronique, and the Laboratoire Traitement et Communication de l'Information, LTCI Unité Mixte de Recherche (UMR) 5141, Ecole Nationale Supérieure des Télécommunications (TELECOM ParisTech), Centre National de la Recherche Scientifique (CNRS), Paris 75013, France (e-mail: qxu@enst.fr; gallion@enst.fr).

A. A. Mondragón and F. J. Mendieta are with the Department of Electronics and Telecommunications, Centro de Investigacion Cientifica y de Educacion Superior de Ensenada (CICESE) Research Center, Ensenada 22800, Mexico (e-mail: arvizu@cicese.mx; mendieta@cicese.mx).

Color versions of one or more of the figures in this paper are available online at http://ieeexplore.ieee.org.

Digital Object Identifier 10.1109/JSTQE.2009.2023803

Balanced homodyne detection (BHD) using standard p-i-n photodiodes and a strong local oscillator (LO), whose noise has only negligible influence, measures only one quadrature since there is no additional noise other than the zero-point fluctuation of the received signal field. Therefore, the output noise is dominated only by vacuum fluctuation entering in the signal port, and a standard quantum-limited (SQL) reception is attained [7], [8].

With these advantages, homodyne detection is also attractive in other applications that are presently of high research interest, such as coherent sensors, coherent reflectometry, coherent spectral analysis, and multiport optical networks. Additionally, the characteristics of highly selective spatial filtering for background radiation rejection are essential in free-space communications and lidar applications.

However, since homodyne detection is sensitive to the instantaneous field complex amplitude, the reception relies on the accurate synchronization of the optical carrier phase with respect to the LO, in the presence of fluctuations due to the inherent linewidth of the signal and LO, as well as the fluctuations in the thermomechanical state of the fiber and other in-line components. For pilot carrier systems, a diversity of feedback tracking configurations have been reported in the conventional configuration of optical phase-locked loops in current-controlled oscillator configurations, and even in injection locking schemes [9], [10].

Efficient transmission requires constellations with suppressed carrier, and the extraction of the phase error constitutes a difficult task that frequently requires nonlinear operations on the post-detection signal(s) and diverse demodulation/tracking schemes such as Costas loops and directed decision loops. The feedback or feedforward (intradyne) configurations [11], [12] have been reported for the reception of classical light fields, carrying high photon number per bit.

Now, carrier phase tracking in homodyne reception imposes further challenges in new applications that operate with very few average photons per observation time such as quantum cryptography [13], long-distance free-space communications and lidar [14], and the other instrumentation and scientific applications that work with photon numbers substantially lower than those used in classical transmission, such as weak coherent states (WCSs).

In this paper, after briefly reviewing the principles of the four-port BHD for single-quadrature measurements and of the eight-port optical hybrid detection for two-quadrature measurements, we present a receiver for the sequential detection of the in-phase (I) and the quadrature (Q) components of a WCS signal that is modulated in a suppressed carrier format, for applications in

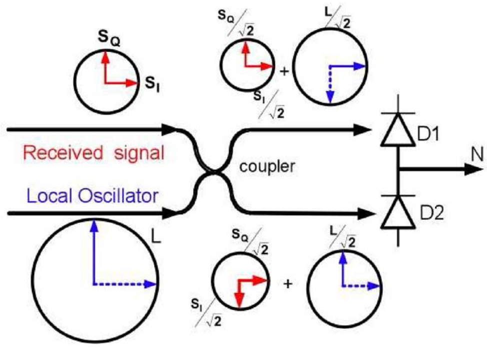

Fig. 1. BHD for two possible phase states of the LO: 90° (solid line) and 0° (dotted line).

the optical communications and cryptography. It uses a single balanced homodyne detector with an LO, whose phase is periodically switched between 0 and $\pi/2$ to alternatively beat with the incoming signal. This constitutes a sequential Costas-loop-type demodulation/synchronization scheme, and we present the postdetection feedback subsystem that is designed for the optical phase carrier tracking. We implement this structure in an experimental homodyne setup for the sequential detection of low photon number and binary phase-modulated optical signals, by applying a signal phase-tracking algorithm. Finally, we present the measurements on its optical phase-tracking characteristics, its postdetection statistics with respect to the uncertainty limits, and its BER performance with respect to the SQL.

II. Four-Port BHD

Fig. 1 shows a general BHD scheme for an incoming signal (red phasor) with a LO (blue phasor), both in a single spatial mode, described by the photon annihilation operators $\hat{a}_S$ and $\hat{a}_L$, respectively, such as the Hermitian field operators with the central carrier frequencies ν_S and ν_L. The instantaneous phases $\phi_S(t)$ and $\phi_L(t)$ are described, respectively, by

$$\hat{E}_S(t) = \sqrt{\frac{h\nu_S}{T}} \begin{bmatrix} \hat{a}_S(t)\exp[j(2\pi\nu_S t + \phi_S(t))] \\ +\hat{a}_S^{+}(t)\exp[-j(2\pi\nu_S t + \phi_S(t))] \end{bmatrix} \quad (1)$$

$$\hat{E}_L(t) = \sqrt{\frac{h\nu_L}{T}} \begin{bmatrix} \hat{a}_L(t)\exp[j(2\pi\nu_L t + \phi_L(t))] \\ +\hat{a}_L^{+}(t)\exp[-j(2\pi\nu_L t + \phi_L(t))] \end{bmatrix} \quad (2)$$

where $\hat{a}_S^{+}$ and $\hat{a}_L^{+}$ are the corresponding adjoint operators, the time duration T is the observation time that is much longer than the optical period but much smaller than the coherence time of the optical source, and h is the Planck's constant.

For the derivation of the number operators resulting from the BHD, *a priori* assumptions on the phase noise processes ϕ_S and ϕ_L are not necessary. They can be considered as usual Wiener process in which the time constant T is much longer than the modulation period. They may be totally uncorrelated if they are issued from different laser sources, or partially correlated if only one source is used in a delayed interferometer configuration, i.e., self-homodyne.

In a scalar analysis, the annihilation operators are expressed in terms of their in-phase (I) and quadrature (Q) Hermitian components: $\hat{a}_S = \hat{a}_{SI} + j\hat{a}_{SQ}$ and $\hat{a}_L = \hat{a}_{LI} + j\hat{a}_{LQ}$. Assume that the signal and the LO are in Glauber's coherent states, and are denoted by $|\alpha_S\rangle$ and $|\alpha_L\rangle$, respectively. For a signal with constant envelope modulation, we can separate the classical and the quantum contributions for the two quadratures in the following form:

$$a_{SI/SQ} = \langle \hat{a}_{SI/SQ}\rangle + \Delta\hat{a}_{SI/SQ} \quad (3)$$

$$\hat{a}_{LI/LQ} = \langle \hat{a}_{LI/LQ}\rangle + \Delta\hat{a}_{LI/LQ} \quad (4)$$

corresponding to the average signal and LO photon numbers as

$$N_S = \langle \hat{a}_S^{+}\hat{a}_S\rangle = |\alpha_{\mathrm{S}}|^2 = \langle \hat{a}_{SI}\rangle^2 + \langle \hat{a}_{SQ}\rangle^2 \quad (5)$$

$$N_L = \langle \hat{a}_L^{+}\hat{a}_L\rangle = |\alpha_{\mathrm{L}}|^2 = \langle \hat{a}_{LI}\rangle^2 + \langle \hat{a}_{LQ}\rangle^2. \quad (6)$$

Furthermore, the variances are

$$\langle \Delta\hat{a}_{SI}^2\rangle = \langle(\hat{a}_{SI} - \langle\hat{a}_{SI}\rangle)^2\rangle \quad (7)$$

$$\langle \Delta\hat{a}_{SQ}^2\rangle = \langle(\hat{a}_{SQ} - \langle\hat{a}_{SQ}\rangle)^2\rangle. \quad (8)$$

Also, the two noncommutating observables are subject to the Heisenberg uncertainty relation given by

$$\langle \Delta\hat{a}_{SI}^2\rangle\langle \Delta\hat{a}_{SQ}^2\rangle \geq \frac{1}{16}. \quad (9)$$

In our case, a coherent state is a minimum uncertainty state for which the standard deviations are $\langle \Delta\hat{a}_{SI}^2\rangle^{1/2} = \langle \Delta\hat{a}_{SQ}^2\rangle^{1/2} = 1/2$, bounded by the zero-point fluctuation energy [15].

In this four-port homodyne detector, the LO is in a coherent state with a large number of photons, then the measured count difference is related to the field strength probability of the signal [16]: for coherent states, the probability density functions (PDFs) of the outcomes of the independent measurements on the in-phase and quadrature components are both Gaussian functions with standard deviation 1/2, which is given by

$$p(\hat{a}_{SI/SQ}) = \sqrt{\frac{2}{\pi}}\exp[-2(\hat{a}_{SI/SQ} - \langle\hat{a}_{SI/SQ}\rangle)^2]. \quad (10)$$

Assuming a lossless and a perfectly balanced coupler, and that the photodetectors are of unit quantum efficiency, due to the coherent subtraction of the two photocurrents, the electron number operator at the output is given by the projection of the signal operator on the quadrature local field operator [17].

As in Fig. 1, to detect $\langle\hat{a}_{SI}\rangle$ (or $\langle\hat{a}_{SQ}\rangle$), we set $\langle\hat{a}_{LI}\rangle$ (or $\langle\hat{a}_{LQ}\rangle$) to zero, as shown in solid (dotted) line in Fig. 1. For example, in the detection of $\langle\hat{a}_{SI}\rangle$ with a strong LO of which $N_L = \langle\hat{a}_{LQ}\rangle^2 \gg N_S$, the dominant term at the BHD output is

$$\hat{N} = 2\langle\hat{a}_{LQ}\rangle(\langle\hat{a}_{SI}\rangle + \Delta\hat{a}_{SI}). \quad (11)$$

The quadrature $\langle\hat{a}_{SI}\rangle$ and its additional quantum noise $\Delta\hat{a}_{SI}$ are amplified by the deterministic part of the quadrature LO component, as a noise-free mixing gain. In this case, only one quadrature is measured, and the input signal quantum noise is the only noise limitation; furthermore, both the LO quantum noise and the excess noises are cancelled.

Then, assuming a perfectly phase-matched LO, the photon number operator can be cast in the form

$$\hat{N} = \langle \hat{N} \rangle + \Delta \hat{N}. \tag{12}$$

We also assume that the signal and the LO are coherent states, denoted $|\alpha_S\rangle$ and $|\alpha_L\rangle$, respectively, and that a constant envelope modulation is used for the signal, and thus, we can obtain the averaged square of the signal photon number, corresponding to the average post-detection electric power as

$$\langle \hat{N} \rangle^2 = 4 N_L N_S \tag{13}$$

and the averaged square of the photon number fluctuations as

$$\langle (\Delta \hat{N}_L)^2 \rangle = N_L. \tag{14}$$

This term corresponds to the postdetection electric noise power, which is the well-known Poisson fluctuation relationship.

And the SNR is, therefore, given by

$$\mathrm{SNR} = 4 N_S. \tag{15}$$

Although the analysis is readily applicable to higher order modulations, without loss of generality, we consider here the case of optical BPSK in which two equally probable modulated binary symbols (0 and 1) are represented by two antipodal phase states in the signal field (0 and π) that maximize the signal distance, and a constant envelope modulation is used to minimize the signal overlap. When a strong LO field is used with perfect phase alignment, in the absence of thermal noise, the BER is given by [18], [19]

$$\mathrm{BER}(N_S) = \frac{1}{2} erfc(\sqrt{2N_s}) \tag{16}$$

where $erfc[x] = (2/\sqrt{\pi}) \int_x^\infty \exp(-t^2)dt$ is the complementary error function.

III. Eight-Port in-Phase and Quadrature Detection

Efficient modulation formats require a suppressed-carrier optical signal, e.g., BPSK, QPSK, or higher order constellations with equally probable symbols; therefore, the conventional optical phase-tracking schemes such as pilot carrier phase-locked loops (PLLs) are not applicable. Several heuristic strategies for phase synchronization have been proposed and experimentally implemented, such as the use of imperfect modulation [20], phase dithering [21], or the use of synchronization bits [22]. All these schemes, however, cause a reduction of the effective bit rate [23].

For a fully suppressed carrier, the detection of the in-phase (I) and quadrature (Q) components of the signal field is required, and should be performed with diverse coherent schemes, such as Costas loops, directed decision loops, or higher order loops, for QPSK or higher order constellations. Fig. 2 shows a general Costas loop I–Q receiver structure, based on the splitting of one of the interacting fields (in this case, the LO) into its in-phase I and quadrature Q components, as well as on their separate

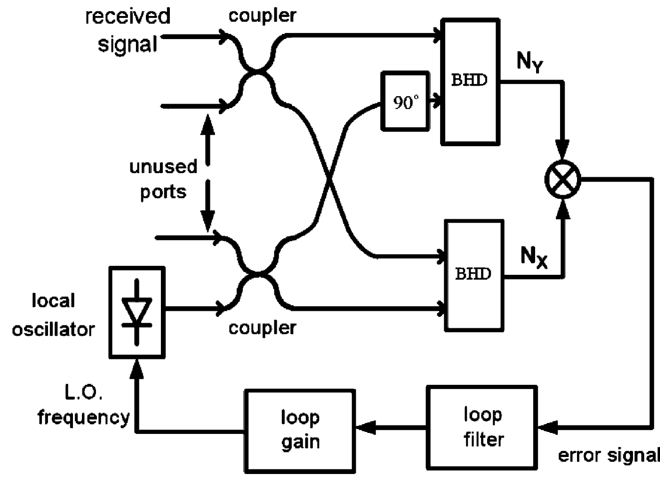

Fig. 2. Optical Costas loop based on a 90° optical hybrid with two BHD receivers. The LO is split and shifted by 90° in the upper branch to beat simultaneously with the in-phase and quadrature components of the signal phasor. The error signal is fed back into the LO for frequency control.

beating with the other optical fields. The purpose of the nonlinear multiplying block is to suppress the modulation [24], leaving only a function of the phase error $\phi_e(t) = \phi_S(t) - \phi_L(t)$ with additive noise to be fed back into the LO frequency, i.e., an optical current-controlled oscillator.

These eight-port structures are extensively used in classical communications for the reception of multilevel phase-shift keying (PSK): QPSK, 8PSK, and also BPSK signals, with tradeoffs related to the power splitting fractions used for data detection and phase lock [25], [26]. Even in the reception of differentially modulated fields, such as DPSK or DQPSK, where demodulation is performed using delayed interferometric configurations [27], they are used to track the relative phase fluctuations due to interferometric drifts, or the source phase noise accumulated during the delay time, etc. [28], [29].

Assuming perfect couplers and detectors characteristics, we use a strong LO with a relative phase θ with respect to the signal field; hence, the number operators at the in-phase (X) and quadrature (Y) outputs can be found as

$$\hat{N}_X = \langle |\hat{a}_L| \rangle [\hat{a}_{SI} \cos(\phi_S - \phi_L) + \hat{a}_{SQ} \sin(\phi_S - \phi_L)] \tag{17}$$
$$\hat{N}_Y = |\langle \hat{a}_L \rangle| [\hat{a}_{SI} \sin(\phi_S - \phi_L) - \hat{a}_{SQ} \cos(\phi_S - \phi_L)]. \tag{18}$$

These operators, corresponding to the SQL, are found to commute, allowing the simultaneous measurement of I and Q signal quadratures for the determination of the optical phase, at the price of introducing vacuum noise through the unused ports. Also, the outcome is in agreement with the uncertainty principle [30], [31].

For coherent states fields, we can separate the classical and quantum contributions for the two photon-number operators as

$$\hat{N}_X = \langle \hat{N}_X \rangle + \Delta \hat{N}_X \tag{19}$$

with $\langle \hat{N}_X \rangle^2 = N_L N_S \cos^2(\phi_S - \phi_L)$ and $\langle (\Delta \hat{N}_X)^2 \rangle = N_L/2$

$$\hat{N}_Y = \langle \hat{N}_Y \rangle + \Delta \hat{N}_Y \qquad (20)$$

with $\langle \hat{N}_Y \rangle^2 = N_L N_S \sin^2(\phi_S - \phi_L)$ and $\langle (\Delta \hat{N}_Y)^2 \rangle = N_L/2$.

Consequently, we can obtain

$$\mathrm{SNR}_X = \mathrm{SNR}_Y = 2N_S. \qquad (21)$$

For the design of the Costas loop, we first express the electrical postdetection signals at the output of the I and Q channels as: $X(t) = \langle X(t) \rangle + \Delta X(t)$ and $Y(t) = \langle Y(t) \rangle + \Delta Y(t)$.

For pulses of duration T_P, the average signals can be expressed, respectively, as

$$\langle X(t) \rangle = R \frac{h\nu}{T_P} \sqrt{N_L N_S}\, \cos(\phi_S - \phi_L) \qquad (22)$$

and

$$\langle Y(t) \rangle = R \frac{h\nu}{T_P} \sqrt{N_L N_S}\, \sin(\phi_S - \phi_L). \qquad (23)$$

Also, the square root fluctuations are

$$\sqrt{\langle \Delta X^2(t) \rangle} = \sqrt{\langle \Delta Y^2(t) \rangle} = R \frac{h\nu}{T_P} \sqrt{\frac{N_L}{2}} \qquad (24)$$

where R is the photodetector responsivity.

With regard to the statistics of the phase noise processes ϕ_S and ϕ_L, for independent signal and LO fields, the in-phase and quadrature photocurrents exhibit the well-known Lorentzian line shape with a full-width half maximum (FWHM) equal to the sum of those of the two lasers; on the other hand, for completely correlated fields, the photocurrent spectrum consists ideally of a Dirac's delta function. As we will describe later, this latter case corresponds to our experiments, using a self-homodyne setup with a relative time delay much smaller than the source coherence time, and the only differential effects consist of the interferometer drifts and technical noises.

For a multiplier gain factor K_m, its output is expressed as a function of the phase error $\phi_e(t) = \phi_S(t) - \phi_L(t)$ [32] as

$$V_m(t) = X(t)Y(t) = \frac{K_m}{2} \left(R \frac{h\nu}{T_P} \right)^2 \sin[2\phi_e(t)] + n_T(t) \qquad (25)$$

where $n_T(t)$ is the resultant noise after multiplication. Now, for the small phase errors, a linear analysis of the Costas loop receiver allows to obtain the phase error statistics, as detailed in Appendix, in which we model the signal and LO phase noises as resulting from finite-lasers linewidth $\Delta\nu$. When a first-order feedback loop with frequency f_n is used, the phase error variance can be obtained, as indicated in Appendix (A14), as

$$\sigma_e^2 = \frac{\Delta\nu}{\sqrt{2} f_n} + \frac{3\pi T_P f_n}{2\sqrt{2} N_S}. \qquad (26)$$

This represents a tradeoff between the phase noise and quantum noise effects [33]. The larger the loop bandwidth, the faster the system tracks the signal phase, but the noisier the feedback. Thus, an optimum bandwidth can be easily found from this equation, as indicated in Appendix (A15) also, as

$$f_{n_{\mathrm{opt}}} = \sqrt{\frac{2\Delta\nu N_s}{3\pi T_P}}. \qquad (27)$$

IV. Sequential In-Phase and Quadrature Detection

Coherent detection, in general, requires very low "linewidth-times-bit period" products in high bit rate systems, i.e., in Gbps range, in order to remain far beyond the noise floor induced by laser phase noise. As well, for the mixing of the LO with the suppressed carrier signal in coherent receivers, diverse optical structures can be used for the optical hybrids [34], for example, the 3-dB couplers and phase delay, the multimode interference filters, or the 3-dB couplers and the polarization components. However, their stabilization is a difficult task, in that the electrooptic phase delay includes several dc control points that must operate in a feedback loop, sharing resources with the modulated data, especially for those applications where the signal average photon number is very low, such as coherent sensing and reflectometry, long-distance space transmission, as well as quantum cryptography.In these applications, the bit rate is often at 1–100 Mbps range; hence, the low "linewidth-times-bit period" product is not relaxed.

Therefore, alternative schemes that do not require the optical 90° hybrid but only one BHD receiver have been proposed, such as the use of deterministic time-switching phase diversity at the receiver end [35] or at the transmitter end [36]. In these schemes, each information bit is replicated, and the incoming signal is alternatively beaten with the in-phase and quadrature components of the LO. For this task, the LO phase is periodically switched between 0° and 90°, in synchronization with the received symbol train. These schemes are simpler to implement, employing only one BHD; however, two transmitted symbols per bit are required, producing a bit rate penalty of 1/2. A more favorable tradeoff in bit rate penalty can be obtained if synchronization bits are inserted at longer intervals [22], [23], as in many cases, the phase process to be tracked is slowly varying.

Applications in quantum communications and cryptography can afford the tradeoff in bit rate, since carrier phase tracking must be performed from low photon number fields with suppressed carrier modulations [37], [38]. For example, for the quantum channel, a sequential measurement based on a couple of independent homodyne measurements of commuting quadratures has been proposed: every measurement is prepared in the same input state before the detection step, within the source's coherence time [39].

Fig. 3 shows a BHD receiver structure for WCSs detection with suppressed carrier: the phase of the LO field is alternatively switched with an electrooptical modulator to sequentially beat with the corresponding received signal symbol [40]. This constitutes a "synthetic Costas loop" that requires only one BHD receiver.

The signal processor block that is detailed in Fig. 4 performs the data sampling and acquisition, sequential I/Q sampling, loop filtering and gain, and digital-to-analog conversion stage (DAC)

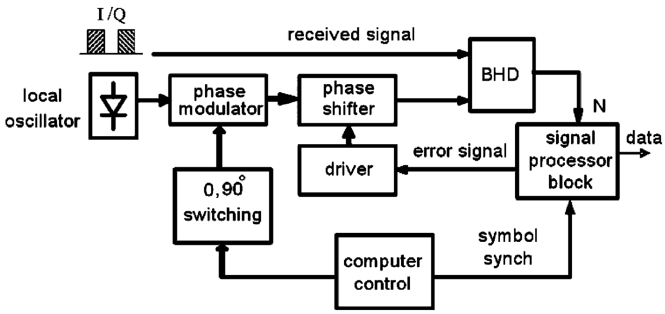

Fig. 3. Costas loop employing an LO with alternate quadratures. The received signal symbols are replicated to beat sequentially with the LO whose phase is switched between 0° and 90° at the symbol rate. Two symbols per bit are required, but only one BHD receiver is needed.

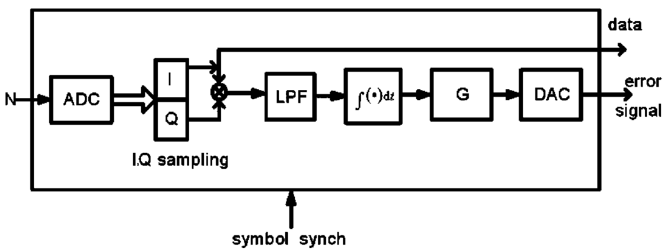

Fig. 4. Elements of the signal processor block as indicated in Fig. 3. LPF: low-pass filter, G: gain.

to generate the error signal to be fed back onto the LO phase using a phase shifter (PS), i.e., a piezoelectric actuator for wide dynamic range and slow phase tracking [41], or a superimposed voltage on the electrooptical modulator for faster phase tracking, but with much narrower dynamic range.

In Appendix, we show the design of the digital Costas loop. We use the equations (A4), (A6), (A7), and a damping factor $\varsigma = 1/\sqrt{2}$ to determine the time constants of the low-pass filter transfer function in the analog domain. Then, by using the Tustin transform, we obtain the corresponding function in the z-domain with the sampling period T_S as

$$F_{\mathrm{LPF}}(z) = \frac{B + Cz^{-1}}{1 - z^{-1}} \tag{28}$$

where the filter constants are $B = (T_S + 2\delta_2)/2\delta_1$ and $C = (T_S - 2\delta_2)/2\delta_1$, also δ_1 and δ_2 are $\delta_1 = \frac{3T_S G}{8\pi\Delta\nu} R(h\nu/T_P)^2 N_L$ and $\delta_2 = (4\pi\Delta\nu N_S/3T_P)^{-1/2}$.

We similarly proceed for the loop integrator as

$$F_{\mathrm{INT}}(z) = \frac{T_S}{2}\frac{1 + z^{-1}}{1 - z^{-1}}. \tag{29}$$

In order to implement our digital Costas loop, we use the inverse Z transform to obtain the corresponding recursive difference equations, which we program in our signal processing block.

V. Experimental Setup and Results

We present in Fig. 5 the experimental setup at the telecommunications wavelength 1550 nm. In this experiment, we use an interferometric arrangement in order to avoid the problem of

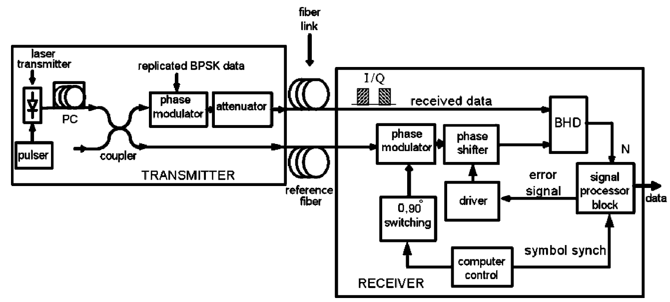

Fig. 5. Experimental setup: at the transmitter, the laser pulses are BPSK-modulated with symbol replication, and strongly attenuated to produce WCS. The signal processor block generates the error signal to track the LO phase with a piezoelectric PS. (PC: polarization controller).

automatic frequency control. This self-homodyne scheme also helps us to generate a baseband signal with narrow spectral spread, even though our laser intrinsic linewidth is of the order of several megahertz, since a conventional DFB telecommunications laser is used.

At the transmitter end, we use a 1550-nm integrated laser electroabsorption modulator (ILM) to generate pulses of 5 ns at 16 MHz repetition rates, which is then split by a polarization splitting coupler. The lower fiber arm provides the continuous wave (CW) LO as the reference, and the upper arm constitutes the information signal that is modulated in BPSK format with an electrooptical modulator, on which we replicate each information bit, and the separation of two consecutive pulses is thus 57.5 ns. The WCS pulses are then generated by strong attenuation on the inline attenuator.

As for a prototype system experiment, our interferometer, including the signal fiber link and the reference fiber link, is constructed with polarization maintaining components to avoid polarization-related impairments. Also, the fiber nonlinearity, dispersion, and amplified spontaneous emission (ASE) noise are considered minor effects since our premier objective is to investigate the phenomena due to the quantum noise. The signal transmission distance is 10 m, and the relative time delay between the signal and the LO is carefully adjusted to around zero by balancing the interferometer, only with some residual time delay that is much smaller than the source coherence time.

At the receiver end, the LO phase is switched alternatively between 0 and $\pi/2$ with another electrooptical modulator, in order to beat sequentially with the I and Q components of the incoming BPSK signal in a BHD receiver that uses InGaAs p-i-n photodiodes followed by an electronic preamplification. The receiver's effective passband is determined by the balanced photoreceiver's bandwidth, i.e., 150 MHz.

At the signal processing block, after A/D converter, only the I signals are retained as data, while both the I and Q signals are used for the digital synthetic Costas loop processing. As the I and Q optical signals are sampled sequentially in an alternate way, a time delay is required in order to perform the multiplication. This block and the subsequent operations, as described in Fig. 4, are implemented in discrete time, with our computer-based algorithm written in C language.

This Costas loop is a simplified version of the maximum *a posteriori* probability (MAP) suppressed carrier BPSK phase estimator for the classical channel [42]. Now, in a conventional Costas loop, an error signal is generated to control the phase of an optical voltage-controlled oscillator (VCO), but in our self-homodyne configuration, we use an optical PS to continuously synchronize the phase of the LO arm. In this synthetic loop, we incorporate an equivalent integration function of the optical VCO using an additional discrete time integrator.

Finally, the resultant phase error signal is fed back via a piezodriver on the PS to force the relative phase to zero. The piezodriver delivers a wide voltage range [−10, 150 V] required for the optical PS whose half-wavelength voltage V_π is 9.95 V, to obtain an operational range of $[-8\pi, 8\pi]$ without reset. The feedback loop bandwidth is 1 kHz that is limited by the processor speed and the piezodriver response time.

We also note that for a long-distance transmission system in which constructing a separate reference fiber link is impractical, an injection-locked laser would be necessary [9], [10]. If an external LO is used, we could redesign our Costas loop with the new parameters, with the tradeoffs as indicated in Appendix. In order to implement a loop to track these broadband fluctuations, we would have to use a faster processor, but the algorithm would not be significantly different. Furthermore, polarization control is mandatory for a coherent optical system, and can be conducted by a polarization diversity receiver scheme. In a single BHD scheme, a polarization stabilizer should be used at the transmitter's side, together with a polarization-tracking loop at the receiver's side.

In the experiments, we first characterized the long-term behavior of the phase error due to the interferometer phase drift induced by the environmental variations, and we have measured a maximal phase drift of 10π per hour under normal laboratory environment. In Fig. 6, we show the error signal in open loop (upper curve) and closed loop (lower curve), obtaining a good stability over several hours.

Next, we performed the measurements on the statistics of the postdetection signal resulting from the received BPSK-modulated signal field for different average photon numbers per pulse, i.e., between 0.1 and 10, beating with strong LO pulses of 4×10^6 photons. In Fig. 7, we show the histograms corresponding to the measured in-phase and quadrature signals for photon numbers of $N_S = 0.5$ (upper curve) and $N_S = 1.5$ (lower curve), in which (I_0 and Q_0) correspond to the fields of phase "0," and (I_π and Q_π) correspond to the fields of phase "π."

Fig. 8 shows the normalized standard deviations for the I and Q component measurements as a function of the signal photon number.

The normalized standard deviations are bounded by the Heisenberg uncertainty principle [43], [44]; however, they increase with N_S, probably due to the excess noise compared to the vacuum fluctuations [45], [46]. In the Q component, our measurements are closer to the zero-point fluctuations, and in the I field, there is more additional noise, especially at high N_S. These impairments are probably caused by the imperfect laser source used in our experiments that does not generate perfect co-

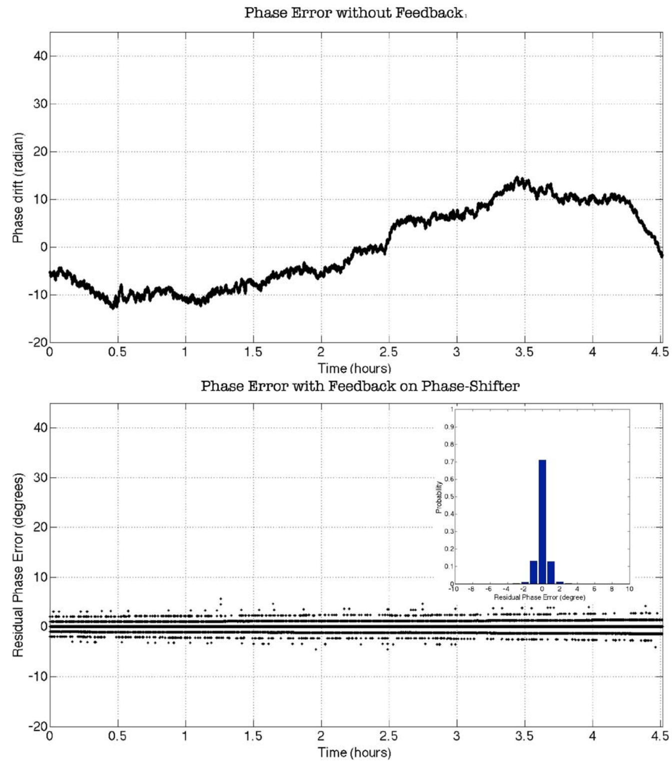

Fig. 6. Long-term behavior of the phase error, in an open loop and in a closed loop.

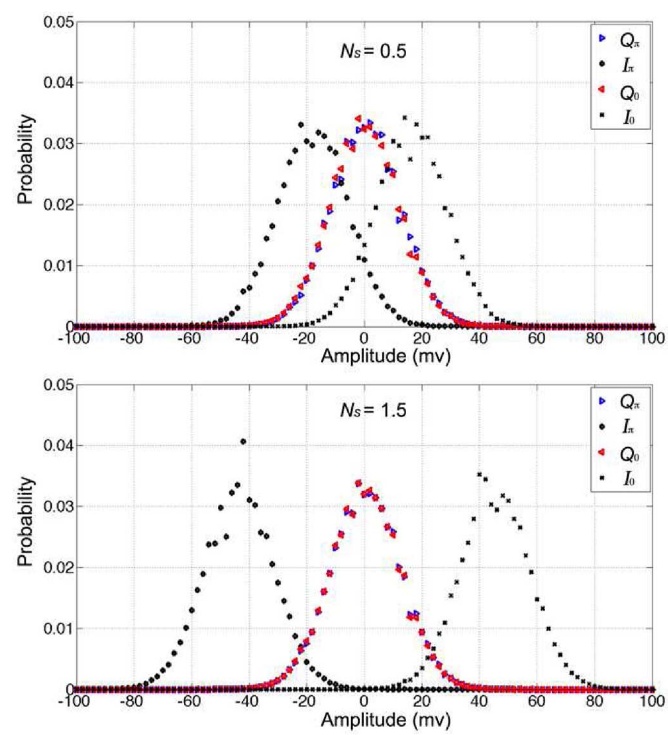

Fig. 7. Histograms of the received I and Q signals for two average photon numbers: $N_S = 0.5$ (upper curves) and $N_S = 1.5$ (lower curves).

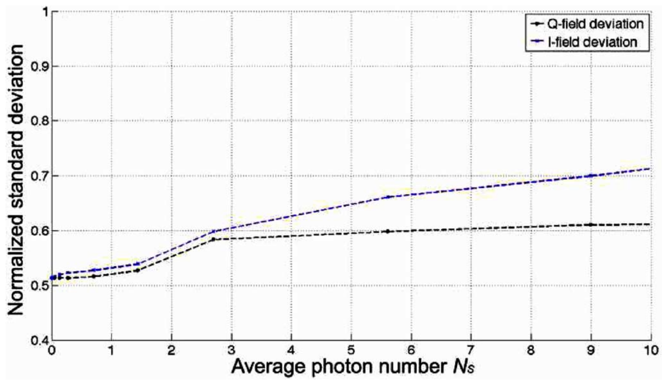

Fig. 8. Standard deviations of the measured I and Q fields.

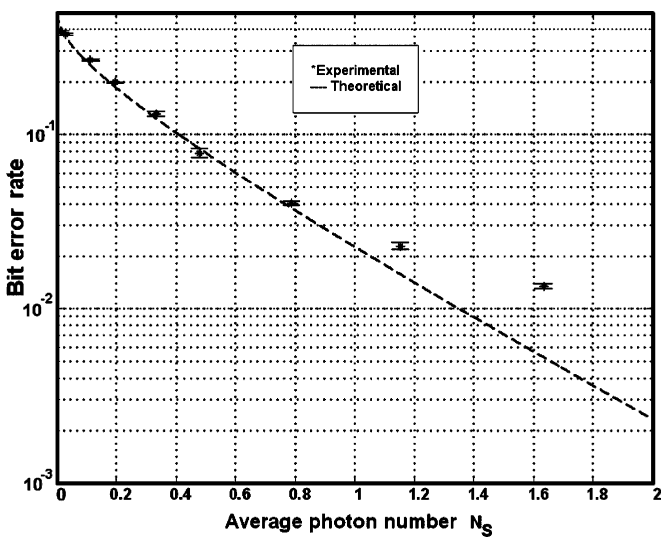

Fig. 9. BER as a function of the signal photon number: experimental measurement (points) and theoretical result (dotted line).

herent states, as well as the residual polarization mismatch and the uneven photodiodes quantum efficiency used in the BHD receiver. Other possible impairments consist of the circuits and amplifier noise, the slow filter response time, and the quantification errors of the analog-to-digital conversion (ADC) stage.

Finally, we performed the BER measurements, using the programming capabilities of our signal processor.

Fig. 9 is a plot of the experimental BER measurements (points) and the theoretical BER (dotted line), as described by the theoretical result equation (16). As in the standard deviation measurements, the weaker the quantum state, the closer is the measurement to the SQL.

VI. Conclusion

Access to the optical carrier phase is important in a diversity of applications, not only in coherent telecommunications but also in other fields such a coherent optical sensor and instrumentation, coherent lidar, etc., that require the measurement of the two field quadratures. In general, this task is performed by Costas loops or decision driven loops that detect both field quadratures simultaneously, requiring two BHD receivers. In these schemes, additional measurement uncertainty is introduced due to the vacuum fields that leak through the unused ports.

The optical receiver implemented in this paper requires only one balanced homodyne detector: it possesses the advantage of noise-free conversion gain, bounded only by the vacuum fluctuations entering at the signal port, and no additional uncertainty is produced.

However, since only one quadrature is measured, we implemented a receiver structure in which a sequential measurement scheme alternatively switches the LO phase between 0° and 90° to sequentially beat with the signal. The signal is prepared in a format that a given bit is replicated, producing, of course, a bit rate penalty of 1/2. But there are diverse applications that are tolerant to this tradeoff, rather than to the noise tradeoff in the simultaneous measurements, i.e., a 3-dB penalty in received optical average photon number.

Our application was in the detection of WCS signals with modulation formats that do not provide an explicit component at the carrier frequency; therefore, phase information must be extracted from the WCS itself, in order to provide an error signal for the phase tracking.

The structure can be applied to the binary format as well as higher order phase modulations. In this paper, we implemented an experimental setup using BPSK modulation, which, for symmetrical constellation, generates a suppressed carrier. We implemented our digital Costas loop in the signal processor block, and obtained good long-term stability.

The measurements on the postdetection statistics were close to the uncertainty limit, especially for small values of the photon number. Similarly, our measurements of BER were close to the SQL for low photon numbers. These results are interpreted as that the attenuation of optical signal power smoothes out the excess noise and the strongly attenuated pulses approach to the coherent states model.

Our system setup is based on an interferometric self-homodyne configuration, which substantially relaxes the speed in the signal processor block, since the strong cross-correlation between the signal and the LO fields yields a very narrow-band postdetection process at baseband. Using an external LO would require, accordingly, a faster processor due to the increasing Costas loop bandwidth for phase locking and the more complex polarization-tracking scheme. This constitutes an interesting research subject for low photon number signals, since the study of the "linewidth-times-bit period" has not been investigated as deeply as in the high-speed, low-BER systems. Finally, the present advances in processor speed will surely allow the implementation of this kind of receivers for uncorrelated fields, providing additional capabilities for the mitigation of the optical channel impairments.

Appendix

Following [47] and [48], we show in Fig. 10 the linear model using a small signal approximation.

We express the equation of the voltage gain V as

$$V_m(t) = A_{PL}\phi_e(t) + n_T(t) \tag{A1}$$

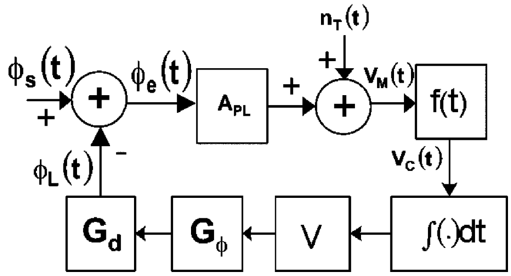

Fig. 10. Small signal model of the optical Costas loop. A_{PL}: multiplication factor, $f(t)$: low-pass filter, G_ϕ: PS gain conversion, G_d: driver voltage gain, and V: voltage gain.

with $A_{PL} = K_m(R(h\nu/T_P))^2 N_L N_S$.

Using this model, we obtain the phase error in the frequency domain as

$$\phi_e(f) = [1 - H_{\mathrm{PLL}}(f)]\phi_i(f) + n_T(f)\frac{H_{\mathrm{PLL}}(f)}{A_{PL}} \tag{A2}$$

where

$$H_{\mathrm{PLL}}(f) = \frac{A_{PL} V G_\phi G_d F(f)}{j2\pi f + A_{PL} V G_\phi G_d F(f)}. \tag{A3}$$

We use a low-pass filter with the time constants τ_1 and τ_2, and the transfer function to obtain

$$F(f) = \Im\{f(t)\} = \frac{1 + j2\pi f \tau_2}{j2\pi f \tau_1} \tag{A4}$$

with $s = j2\pi f$ and $\omega_n = 2\pi f_n$, we obtain

$$H_{\mathrm{PLL}}(s) = \frac{2\zeta\omega_n s + \omega_n^2}{s^2 + 2\zeta\omega_n s + \omega_n^2} \tag{A5}$$

where the natural frequency is

$$f_n = \frac{1}{2\pi}\sqrt{\frac{A_{PL} V G_\phi G_d}{\tau_1}}. \tag{A6}$$

And the damping factor is

$$\zeta = \pi f_n \tau_2. \tag{A7}$$

Our main objective is to minimize the phase error variance σ_e^2, expressed with the help of the (A2) as follows:

$$\sigma_e^2 = \sigma_{\mathrm{PN}}^2 + \sigma_{nT}^2. \tag{A8}$$

The first term in the right-hand side (RHS) is due to the lasers phase noise and the second term corresponds to the quantum noise.

The phase noise contribution due to the laser linewidth $\Delta\nu$ is

$$\sigma_{\mathrm{PN}}^2(f) = \int_{-\infty}^{\infty} G_{\dot{\phi}N}(f)[1 - H_{\mathrm{PLL}}(f)]^2 df. \tag{A9}$$

Using the integration in Fourier domain, we can have

$$\frac{G_{\dot{\phi}N}(f)}{j2\pi f} = G_{\mathrm{PN}}(f) = \frac{\Delta\nu}{\pi f^2}. \tag{A10}$$

Resulting in

$$\sigma_{\mathrm{PN}}^2(f) = \frac{\Delta\nu}{2\varsigma f_n}. \tag{A11}$$

While the quantum noise contribution is

$$\sigma_{nT}^2(f) = \frac{1}{A_{PL}^2}\int_{-\infty}^{\infty} G_{n_T}(f)[H_{\mathrm{PLL}}(f)]^2 df. \tag{A12}$$

If we assume that the total additive noise is Gaussian with white power spectral density, we can obtain

$$\sigma_{nT}^2(f) = \frac{T_P \pi f_n}{N_S}\left(\frac{1 + 4\varsigma^2}{4\varsigma}\right). \tag{A13}$$

Finally, by choosing $\varsigma = 1/\sqrt{2}$. we obtain the total phase error variance as

$$\sigma_e^2 = \frac{\Delta\nu}{\sqrt{2} f_n} + \frac{3\pi T_P f_n}{2\sqrt{2} N_S}. \tag{A14}$$

We find that the optimal value of the natural frequency that minimizes σ_e^2 can be expressed as

$$f_{n_{\mathrm{opt}}} = \sqrt{\frac{2\Delta\nu N_S}{3\pi T_P}}. \tag{A15}$$

Acknowledgment

The authors would like to acknowledge Avanex for the loan for the 1550-nm integrated laser modulator module.

References

[1] L. G. Kazovsky, G. Kalogerakis, and W. T. Shaw, "Homodyne phase-shift-keying systems: Past challenges and future opportunities," *J. Lightw. Technol.*, vol. 24, no. 12, pp. 4876–4884, Dec. 2006.

[2] A. H. Gnauck and P. J. Winzer, "Optical phase shift keyed transmission," *J. Lightw. Technol.*, vol. 23, no. 1, pp. 115–130, Jan. 2005.

[3] K. P. Ho, *Phase Modulated Optical Communication Systems*. Berlin, Germany: Springer-Verlag, 2005.

[4] P. P. Mitra and J. B. Stark, "Nonlinear limit to the information capacity of optical fibre communications," *Nature*, vol. 411, pp. 1027–1030, 2001.

[5] J. M. Kahn and K. P. Ho, "A bottleneck for optical fibers," *Nature*, vol. 411, pp. 1007–1010, 2001.

[6] H. P. Yuen and V. W. S. Chan, "Noise in homodyne and heterodyne detection," *Opt. Lett.*, vol. 8, pp. 177–179, 1983.

[7] B. L. Schumaker, "Noise in homodyne detection," *Opt. Lett.*, vol. 9, pp. 189–191, 1982.

[8] M. J. Collett, R. Loudon, and C. W. Gardiner, "Quantum theory of optical homodyne and heterodyne detection," *J. Mod. Opt.*, vol. 34, pp. 881–902, 1987.

[9] A. C. Bordonalli, C. Walton, and A. J. Seeds, "High-performance phase locking of wide line width semiconductor lasers by combined use of optical injection locking and optical phase locked loop," *J. Lightw. Technol.*, vol. 17, no. 2, pp. 328–342, Feb. 1999.

[10] I. Petitbon, P. Gallion, G. Debarge, and C. Chabran, "Locking bandwidth and relaxation oscillations of an injection-locked semiconductor laser," *IEEE J. Quantum Electron. (JQE)*, vol. 24, no. 2, pp. 148–154, Feb. 1988.

[11] R. Noe, "Phase noise tolerant synchronous QPSK/BPSK baseband-type intradyne receiver concept with feedforward carrier recovery," *J. Lightw. Technol.*, vol. 23, no. 2, pp. 802–808, Feb. 2005.

[12] K. Kikuchi, "Phase diversity homodyne detection of multilevel optical modulation with digital carrier phase estimation," *IEEE J. Sel. Topics Quantum Electron.*, vol. 12, no. 4, pp. 563–570, Jul./Aug. 2006.

[13] N. Gisin, G. Ribordy, W. Tittel, and H. Zbinden, "Quantum cryptography," *Rev. Mod. Phys.*, vol. 74, pp. 145–195, 2002.

[14] V. W. S. Chan, "Free space optical communications," *J. Lightw. Technol.*, vol. 24, no. 12, pp. 4750–4762, Dec. 2006.

[15] J. H. Shapiro, S. R. Shepard, and N. C. Wong, "Ultimate quantum limits on phase measurement," *Phy. Rev. Lett.*, vol. 62, pp. 2377–2380, 1989.

[16] W. Vogel and D. G. Welsch, *Lectures on Quantum Optics*. Berlin, Germany: Akademie Verlag, 1994, ch. 4.

[17] P. Gallion, F. Mendieta, and S. Jiang, "Signal and quantum noise in optical communications and cryptography," in *Progress in Optics,* E. Wolf, Ed., 2009, vol. 52, pp. 149–259, ch. 3.
[18] G. P. Agrawal, *Fiber-Optic Communication Systems*, 3rd ed. New York: Wiley-Interscience, 2002, ch. 10.
[19] J. Salz, "Coherent lightwave communications," *AT& T Tech. J.*, vol. 10, pp. 2153–2209, 1985.
[20] W. Glatt, M. A. Schreiblehner, C. Haider, and W. R. Lebb, "Optical PSK homodyne system using a switched residual carrier for phase synchronization," *Electron. Lett.*, vol. 32, pp. 1386–1387, 1996.
[21] F. Herzog, K. Kudielka, D. Erni, and W. Bachtold, "Optical phase locking by local oscillator phase dithering," *IEEE J. Quantum Electron.*, vol. 42, no. 10, pp. 973–985, Oct. 2006.
[22] B. Wandernoth, "20 photons/bit 565 Mbit/s PSK homodyne receiver using synchronization bits," *Electron. Lett.*, vol. 28, pp. 387–388, 1992.
[23] K. H. Kudielka and W. Klaus, "Optical homodyne PSK receiver: Phase synchronization by maximizing baseband signal power," in *Proc. IEEE LEOS 1999 Soc. Meet.*, pp. 295–296.
[24] I. B. Djordjevic, "Optical homodyne PSK receivers with Costas loop for long-haul communications," *J. Opt. Commun.*, vol. 23, pp. 154–158, 2002.
[25] L. G. Kazovsky, "Balanced phase-locked loops for optical homodyne receivers," *J. Lightw. Technol.*, vol. 4, no. 2, pp. 182–95, Feb. 1986.
[26] S. Norimatsu, "Optimum optical power splitting ratio of decision driven phase locked loop in BPSK homodyne receiver," *J. Lightw. Technol.*, vol. 13, no. 11, pp. 2183–2190, Nov. 1995.
[27] J. M. Kahn, "Spectral efficiency limits and modulation/detection techniques for DWDM systems," *J. Sel. Topics Quantum Electron.*, vol. 10, pp. 259–272, 2004.
[28] P. J. Winzer and R.-J. Essiambre, "Advanced modulation formats for high-capacity optical transport networks," *J. Lightw. Technol.*, vol. 24, no. 12, pp. 4711–4728, Dec. 2006.
[29] C. Xu, X. Liu, and X. Wei, "Differential phase-shift keying for high spectral efficiency optical transmissions," *IEEE J. Sel. Topics in Quantum Electron.*, vol. 10, no. 2, pp. 281–293, Mar./Apr. 2004 (Invited Paper).
[30] N. G. Walker, "Quantum theory of multiport optical homodyning," *Opt. Acta.*, vol. 34, pp. 15–60, 1987.
[31] M. G. Raymer, J. Cooper, and M. Beck, "Many-port detection of an optical phase," *Phy. Rev. A*, vol. 48, pp. 4617–4628, 1993.
[32] I. B. Djordjevic, M. C. Stefanovic, S. S. Ilic, and G. T. Djordjevic, "An example of a hybrid system: Coherent optical system with Costas loop in receiver-system for transmission in baseband," *J. Lightw. Technol.*, vol. 16, no. 2, pp. 177–183, Feb. 1998.
[33] L. G. Kazovsky, S. Benedetto, and A. Willner, *Optical Fiber Communication Systems*. Boston, MA: Artech House, 1996.
[34] M. Seimetz and C. M. Weinert, "Options, feasibility, and availability of 2×4 90° hybrids for coherent optical systems," *J. Lightw. Technol.*, vol. 24, no. 3, pp. 1317–1322, Mar. 2006.
[35] J. M. Fabrega and J. Prat, "Homodyne receiver prototype with time-switching phase diversity and feed-forward analog processing," *Opt. Lett.*, vol. 32, pp. 463–465, 2007.
[36] L. M. I. Habbab, J. M. Kahn, and J. I. Greenstein, "Phase insensitive zero I.F. coherent optical system using phase switching," *Electron. Lett.*, vol. 24, pp. 974–976, 1988.
[37] T. Hirano, H. Yamanaka, M. Ashikaga, T. Konishi, and R. Namiki, "Quantum cryptography using pulsed homodyne detection," *Phys. Rev. Lett.*, vol. A68, pp. 042331-1–042331-7, 2003.
[38] F. Grosshans, G. Van Assche, J. Wenger, R. Brouri, N. J. Cerf, and P. Grangier, "Quantum key distribution using Gaussian-modulated coherent states," *Nature*, vol. 421, pp. 238–241, 2003.
[39] G. M. D'Ariano, M. G. A. Paris, and R. Seno, *Homodyne Detection of the Phase Through Independent Measurements in Quantum Interferometry*, F. De Martini, G. Denardo, and Y. Shih, Eds. Weinheim, N.Y.: VCH Verlag, 1996, pp. 301–306.
[40] Q. Xu, M. B. Costa e Silva, P. Gallion, and F. J. Mendieta, "Auto-compensating quantum crypto-system using homodyne detection," presented at the Conf. OFC 2008, San Diego, CL.
[41] Q. Xu, M. B. Costa e Silva, A. Arvizu, P. Gallion, and F. J. Mendieta, "Weak coherent state homodyne detection with sequential I-Q measurements," presented at the CLEO, San Jose, CL, 2008.
[42] H. L. Van Trees, *Detection, Estimation, and Modulation Theory*. New York: Wiley–Interscience, 1968.
[43] T. Opatrny, M. Dakna, and D. G. Welsch, "Number-phase uncertainty relations: Verification by balanced homodyne measurement," *Phy. Rev. A*, vol. 57, pp. 2129–2133, 1998.
[44] D. T. Smithey, M. Beck, J. Cooper, and M. G. Raymer, "Measurement of number-phase uncertainties of optical fields," *Phy. Rev.*, vol. A48, pp. 3159–3167, 1993.
[45] J. M. Geremia, "Distinguishing between coherent states with imperfect detection," *Phy. Rev.*, vol. 70, pp. 062303-1–062303-9, 2004.
[46] R. L. Cook, P. J. Martin, and J. M. Geremia, "Optical coherent state discrimination using a real-time closed-loop quantum measurement," *Nature*, vol. 446, pp. 774–777, 2007.
[47] W. C. Lindsey and M. K. Simon, *Telecommunication Systems Engineering*. Englewood Cliffs, NJ: Prentice-Hall, 1973, ch. 11.
[48] M. K. Simon and W. C. Lindsey, "Optimum performance of suppressed carrier receivers with Costas loop tracking," *IEEE Trans. Commun.*, vol. COM-25, no. 2, pp. 215–227, Feb. 1977.

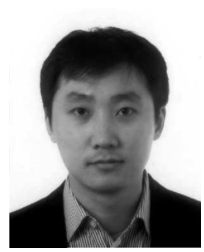

Qing Xu was born in Shanghai, China, on November 15, 1979. He received the B.E. degree in information engineering from Shanghai Jiaotong University, Shanghai, in 2002, the M.E. degree in telecommunications from Ecole Spéciale de Mécanique et d'Electricité, Paris, France, in 2005, and the Ph.D. degree in electrical engineering from Ecole Nationale Supérieure des Télécommunications (ENST) (TELECOM ParisTech), Paris, in 2009. He received the French Government Research Fellowship.

From 2002 to 2003, he was a CDMA R&D Engineer at Wide Telecom, Inc. In 2005, he joined the Département Communications et Electronique, ENST. He is also with the "Laboratoire de Traitement et Communication de l'Information, LTCI," joint research laboratories between ENST and the "Centre National de la Recherche Scientifique" (CNRS). He is now an engineer scientist in ENST engaged in the research on the experimental phase-encoding quantum key distribution system and the coherent detection technologies with the Group of Optical Communications.

Arturo Arvizu Mondragón was born in Mexico City in 1961. He received the B.S.E.E. and M.Eng. degrees in electronics from the Universidad Nacional Autónoma de México, Mexico City, Mexico, in 1985 and 1990, respectively, and the Dr. Eng. degree in telecommunications from the Centro de Investigacion Cientifica y de Educacion Superior de Ensenada (CICESE) Research Center, Ensenada, Mexico, in 2000.

In 1987, he joined the Institute of Electrical Research, Cuernavaca, Mexico, where he was engaged in projects related to the optical and optoelectronics communications systems with application in power generation systems, and laboratories for test, measurement, and characterization of electrical systems. In 1992, he joined the CICESE Research Center, where he is currently involved in the fields of quantum communications, and optical fiber and optical wireless communications with coherent detection. From 2000 to 2001, he was a Postdoctoral Researcher in the Telecommunications Department, École Nationale Supérieure des Télécommunications, Paris, France.

Philippe Gallion (M'82–SM'93) received the "Doctorat de Troisième Cycle" from the University of Rheims, Rheims, France, in 1975, and the "Doctorat d'Etat" from the University of Montpellier, Montpellier, France, in 1986.

Since 1978, he has been with the "Ecole Nationale Supérieure des Télécommunications," ENST, also called "TELECOM ParisTech," Paris, France, where he is currently a Full Professor. He is also the In-Charge of the research activities in the fields of communications, electronics, radio frequencies, and optoelectronics in the "Laboratoire de Traitement et Communication de l'Information, LTCI," joint research laboratories between ENST and the "Centre National de la Recherche Scientifique" (CNRS). He has made pioneering contributions on laser noise, injection locking, semiconductor laser modulation chirp and tuning, coherent systems and optical devices, and digital optical communications systems and networks. His current research interests include theory, design, modeling, and characterization of functional devices, advanced optical digital communication systems and networks, radio over fiber systems, and quantum cryptography systems. He has authored or coauthored more than 200 technical papers and communications, and was the advisor for more than 40 Ph.D. degree dissertations.

Prof. Gallion is a member of the Optical Society of America. He is the Chairman of the IEEE Photonics Society [formerly known as IEEE Laser and Electrooptics Society (LEOS)] French Chapter. He is a member of the Editorial Board and the Scientific Committee of several technical publications, and a member of the Program or Steering Committee of the international scientific meetings.

Francisco J. Mendieta (M'80) received the Bachelor's degree in mechanical and electrical engineering from the National University of Mexico (UNAM), Mexico City, Mexico, the Master's and Doctor's degrees from the National Superior School of Telecommunications (ENST, Telecom Paris Tech), Paris, France, in coherent optical communications.

He was with the Institute for Electrical Research (IIE), Mexico, where he was involved in development projects on applications of optical fibers to electrical power systems. He was with UNAM, where he was the Leader of a continuous education program on telecommunications systems. During a leave at the Utah State University, USA, he participated in a project on instrumentation for space experiments. He formed the Optical Communications Group, and lead several research projects on telecommunications and sensing at the Centro de Investigacion Cientifica y de Educacion Superior de Ensenada (CICESE), Ensenada, Mexico, where he is currently a Lecturer for the Graduate Program on Optical and Digital Telecommunications, and has been an Advisor for diverse Master's and Doctor's thesis. During a sabbatical leave at Telecom ParisTech, France, he was involved in the research on quantum communications and cryptography. He has authored or coauthored diverse journal papers and conference papers in the field of optical communications and sensing.